Failed retrograde transport of NGF in a mouse model of Down's syndrome: Reversal of cholinergic neurodegenerative phenotypes following NGF infusion

Jonathan D. Cooper*[†‡], Ahmad Salehi*[†], Jean-Dominique Delcroix*, Charles L. Howe*, Pavel V. Belichenko*, Jane Chua-Couzens*, Joshua F. Kilbridge*, Elaine J. Carlson[§], Charles J. Epstein[§], and William C. Mobley*

*Department of Neurology and Neurological Sciences and the Program in Neuroscience, Stanford University, Stanford, CA 94305; and [§]Department of Pediatrics, University of California, San Francisco, CA 94143

Age-related degeneration of basal forebrain cholinergic neurons (BFCNs) contributes to cognitive decline in Alzheimer's disease and Down's syndrome. With aging, the partial trisomy 16 (Ts65Dn) mouse model of Down's syndrome exhibited reductions in BFCN size and number and regressive changes in the hippocampal terminal fields of these neurons with respect to diploid controls. The changes were associated with significantly impaired retrograde transport of nerve growth factor (NGF) from the hippocampus to the basal forebrain. Intracerebroventricular NGF infusion reversed well established abnormalities in BFCN size and number and restored the deficit in cholinergic innervation. The findings are evidence that even BFCNs chronically deprived of endogenous NGF respond to an intervention that compensates for defective retrograde transport. We suggest that age-related cholinergic neurodegeneration may be a treatable disorder of failed retrograde NGF signaling.

Basal forebrain cholinergic neurons (BFCNs) undergo atrophy and apparent loss in Alzheimer's disease (AD) (1, 2) and in elderly Down's syndrome (DS) patients (3, 4). Partial trisomy 16 (Ts65Dn) mice are trisomic for the mouse homologue of the so-called Down's syndrome critical region of human chromosome 21 (HSA21) (5). A genetic model for DS, the Ts65Dn mouse provides the opportunity for studying underlying pathophysiological mechanisms. Ts65Dn mice exhibit certain developmental abnormalities that may be analogous to mental retardation (6). Parallels with DS and AD are also apparent. For example, following initial normal development, the basal forebrain of these mice exhibit age-related reductions in the size and number of p75[NGFR]-immunoreactive BFCNs relative to diploid controls (6). These changes are correlated with impaired performance in cognitive tasks that test hippocampal function (7, 8). NGF is a neurotrophic factor whose actions on BFCNs are required for their normal development and function (9). Given the marked similarities in the changes seen in the BFCNs of Ts65Dn mice and those in which animals have been deprived of NGF (10–12) or its receptors (13), we tested the hypothesis that the progressive abnormalities in BFCNs in Ts65Dn mice resulted from impaired NGF signaling. Our results suggest that deficient trophic support, because of failed retrograde transport of the NGF signal, contributes significantly to the neurodegenerative phenotype. They raise the possibility that populations of BFCNs previously presumed to die in DS and AD instead survive in an atrophic state that may be rescued by restoring trophic support to BFCN cell bodies.

Materials and Methods

Studies of BFCN Cell Bodies and Axons. Mice were maintained on a B6C3HF1 outbred background by mating Ts65Dn female mice (originally obtained from The Jackson Laboratory) with B6C3HF1 male mice (The Jackson Laboratory). Fibroblasts or lymphocytes were karyotyped to distinguish Ts65Dn and 2N mice. Male mice were used in all studies. Histological analyses were performed blind to genotype. BFCNs were identified by immunohistochemical staining for p75[NGFR], a neurotrophin receptor localized specifically to cholinergic neurons in the basal forebrain (14). The central nervous system of male Ts65Dn and 2N mice was examined at 6, 12, and 18 months of age. The cell bodies of BFCNs were examined in 2N ($n = 6$) and Ts65Dn ($n = 5$) mice at each age. Mice were deeply anesthetized with sodium pentobarbital (200 mg/kg i.p.) (Abbott) and perfused for subsequent immunohistochemical detection of p75[NGFR] (REX, 1:4,000; L. Reichardt, Univ. of California, San Francisco) in 40 μm free-floating coronal sections through the basal forebrain and hippocampus. All immunostaining was carried out as described (15); for each age or treatment group of Ts65Dn and 2N mice, identical conditions were used. Unbiased stereological methods (Stereologer, Systems Planning & Analysis, Alexandria, VA) were used to determine the number (optical fractionator method) of p75[NGFR]-positive neurons throughout the rostral-caudal extent of the medial septal nucleus (MSN) of each animal (16). The cross-sectional areas of p75[NGFR]-positive neurons randomly sampled throughout the rostral-caudal extent of the MSN were measured as described (15), using an MCID image analysis system (Imaging Research, St. Catherine's, ON, Canada).

To examine cholinergic fibers in the molecular layer of the dentate gyrus and to characterize their distribution, we measured the density of p75[NGFR] immunoreactivity in an optical slice taken immediately ventral to the dentate granule cell layer. First, we measured the thickness of the molecular layer of the dentate gyrus, a representative and anatomically defined hippocampal subfield, using MCID image analysis. For each animal, three to five p75[NGFR]-immunostained sections were examined from the rostral pole of the hippocampus (bregma = -0.94 to -2.30 mm as defined; ref. 17). Within sections, the entire mediolateral extent of the molecular layer in the ventral blade of the dentate gyrus was examined. The optical density of p75[NGFR] immunostaining was measured in optical slices through the molecular

NEUROBIOLOGY

layer that was oriented perpendicular to the granular cell layer (see Fig. 2a) using a 40× objective and Scion Image (Scion, Frederick, MD). We examined 2N and Ts65Dn mice at 6 months (n = 3 each) and at 18 months (n = 5 each). Optical density measurements (0–255 units) were corrected for background by subtracting the density over the optic nerve in the same animal (average background density = 56 units). On average, 20 optical slices were measured in each animal. To correct for the variable width of the molecular layer at different rostrocaudal levels, optical density measurements were sorted into bins, each representing 5% of the length of the optical slice. Data were plotted as mean optical density vs. location in the optical slice.

Studies of NGF Protein, Transport, and Binding. The hippocampus and septal region of Ts65Dn and 2N mice at 6 months (n = 5 each) and 12 months (n = 4 each) of age were dissected and immediately stored on dry ice. Samples were analyzed for NGF protein by using an enzyme-linked immunoabsorbent assay (ELISA) from Boehringer Mannheim as described (18). For transport studies, radiolabeled neurotrophins were prepared. NGF (produced as indicated; ref. 19), BDNF, and NT-3 (Regeneron Pharmaceuticals, Tarrytown, NY) were iodinated to a specific activity of 39, 49, and 72 μCi/μg (1 Ci = 37 GBq), respectively, with a modification of a standard method (20), using IODO-GEN tubes (Pierce). Each neurotrophin, in Tris/BSA iodination buffer (25 mM Tris/400 mM NaCl/0.25% BSA/5 mM EDTA), was adjusted to 0.4 μCi/μl with PBS containing 1 mg/ml BSA and 1 mg/ml glucose. Ts65Dn and 2N mice (n = 3 each) were anesthetized with sodium pentobarbital (60 mg/kg, i.p) and placed in a stereotaxic frame (Kopf Instruments, Tujunga, CA), and 0.3 μl of ^{125}I-neurotrophin solution (containing 0.125 μCi) was injected stereotactically unilaterally into the center of the hippocampal formation [coordinates $x = -3.0$ mm, $y = +3.2$ mm, $z = -3.4$ mm, as defined by Franklin and Paxinos (17)] over 6 min by using a Harvard PHD-2000 infusion pump (Harvard Instruments, Boston, MA) via a fluid-filled tubing system fitted to a 31-gauge metal cannula (Plastics One, Roanoke, VA). The cannula was left in place for an additional 6 min and was withdrawn over 10 min. After 1.5, 3, or 6 h, animals were anesthetized with sodium pentobarbital (200 mg/kg), and the septum, fimbria, hippocampi, and cerebellum were rapidly dissected. Samples of fimbria were dissected from the hippocampus and divided into three equal segments: (i) fimbria 3, close to the hippocampus; (ii) fimbria 1, close to the septum; and (iii) fimbria 2, the intervening segment. The amount of radioactivity in each sample was determined by γ-counting (Beckman 4000, Beckman Coulter). Background radioactivity was determined in the uninjected hippocampus and the cerebellum. The transport of radiolabeled NGF to the septum was effectively abolished by coinjecting a 500-fold excess of unlabeled NGF (data not shown).

For NGF binding studies, the hippocampuses from 12 Ts65Dn and 12 2N mice were collected on ice and immediately placed into ice-cold homogenization buffer (0.32 M ultra pure sucrose/10 mM Tris, pH 7.0). Samples, pooled by genotype, were placed in 10 ml and homogenized by 12 full strokes of a Teflon pestle in a glass homogenizer. The homogenate volume was brought to 24 ml with fresh homogenization buffer, and the homogenate was centrifuged (1,000 × g, 20 min, 4°C). The supernatant was collected and recentrifuged (12,000 × g, 20 min, 4°C) to isolate a crude synaptosomal pellet. The pellet was washed by resuspending in ice-cold PBS, then resuspended in 12 ml of ice-cold binding buffer (PBS with 1 mg/ml BSA/1 mg/ml glucose, pH 7.4). Samples were warmed for 15 min at 37°C, and 12 1-ml aliquots of each genotype were chilled (4°C) while rotating. ^{125}I-NGF (2 nM) was added, and samples were rotated for 1 h at 4°C to permit binding of NGF to surface receptors while inhibiting internalization. To control for nonspecific bind-

ing and internalization, half of the samples were incubated with ^{125}I-NGF in the presence of excess unlabeled NGF (2,000 nM). Samples were either warmed for 15 min at 37°C or left unwarmed for the same period. They were then chilled briefly in a salt-ice water bath and for 10 min on ice. All samples were pelleted by centrifugation (12,000 × g, 1 min, 4°C) and washed briefly in ice-cold PBS. They were then resuspended in 0.2 M acetic acid containing 0.5 M NaCl for 10 min at 4°C to strip surface-bound NGF. Synaptosomes were pelleted by brief centrifugation, and the supernatants and pellets were collected. The pellets, containing internalized NGF, were washed two times in ice-cold PBS and lysed in 0.1 N NaOH. The supernatants represented surface-bound NGF. All samples were assayed in a Beckman gamma counter. Nonspecific binding and internalization averaged 25% of their respective totals; these values were subtracted from the totals to give specific binding and internalization. Internalization was calculated by subtracting specific internalization in unwarmed samples from that in samples warmed for 15 min.

NGF Treatment. Ts65Dn and 2N mice of age 18 months were anesthetized with sodium pentobarbital (60 mg/kg, i.p.), and cannulas attached to Alzet microosmotic minipumps (model 1002, Alza) were implanted into the lateral ventricle at the level of the anterior commissure as described (21). The pumps contained artificial cerebrospinal fluid solution either without NGF (vehicle-treated) (2N = 6; Ts65Dn = 8) or with NGF (0.155 μg/μl; 2N = 6; Ts65Dn = 8); the injection rate was 0.25 μl/h. NGF-treated animals received 0.9 μg of NGF per day. After 2 weeks of treatment, animals were perfused for subsequent immunohistochemical detection of p75^{NGFR}.

Results

BFCN Cell Number and Size. Unbiased stereological methods were used to compare the number of BFCNs in the MSN of male Ts65Dn and diploid (2N; i.e., control) B6C3H mice at 6, 12, and 18 months of age (Fig. 1). There was no significant difference at 6 months of age (Fig. 1a). Conversely, a significant reduction (20%) in the number of p75^{NGFR}-positive BFCNs was present in Ts65Dn vs. 2N at 12 months of age, and this was more marked at 18 months (Fig. 1a). Furthermore, persisting p75^{NGFR}-positive neurons were smaller than in 2N controls at these ages with significant reductions in cross-sectional areas of 7.5% and 15% at 12 and 18 months of age, respectively (Fig. 1b). There was a population-wide effect for the change in cell size and for its progression over time (data not shown). It is noteworthy that the differences between Ts65Dn and 2N mice in number and size resulted in part from a failure of BFCNs in Ts65Dn to undergo the increases seen in 2N. However, there were also regressive changes in BFCNs in Ts65Dn mice that between 6 and 12 months of age resulted in significantly smaller (6.5% decrease; $P = 0.016$) and fewer (13.7% decrease; $P = 0.028$) BFCNs (Fig. 1).

BFCN Projections in the Hippocampus. The distribution of cholinergic fibers in the hippocampus was examined to determine whether changes in BFCN soma were accompanied by age-related changes in their terminal fields. In the molecular layer, a representative region of the hippocampal formation, we noted no change in the pattern of staining at 6 months of age (Fig. 2 a and b). However, at 18 months of age, there was increased staining in the inner portion of this layer in Ts65Dn vs. 2N mice (Fig. 2 c and d). Quantitative methods were used to examine p75^{NGFR}-immunoreactive cholinergic fibers in the molecular layer in Ts65Dn and control mice at 6 and 18 months of age. First, we measured the width of the molecular layer adjacent to the ventral blade of the dentate gyrus (Fig. 2, dotted lines). There were no significant differences between Ts65Dn and 2N mice at 6 months of age (Ts65Dn = 149.8 ± 5.7 μm, mean ±
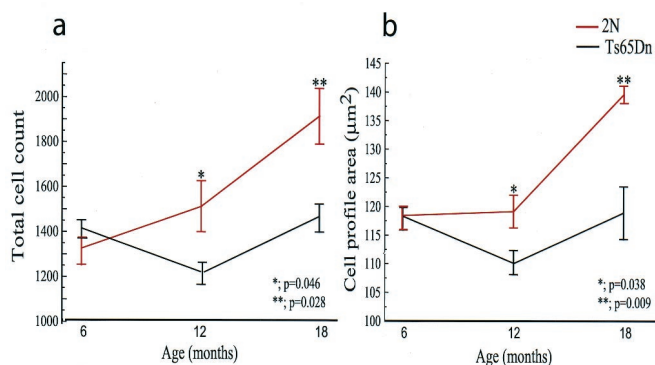
Fig. 1. Age-related abnormalities of BFCNs in Ts65Dn mice. (*a*) Plots of unbiased stereological estimates of the number of p75^{NGFR}-immunoreactive BFCNs in the MSN (mean ± SEM) revealed no significant difference between control (2N, red line) and Ts65Dn mice (black) at 6 months of age (2N = 1328 ± 74; Ts65Dn = 1408 ± 42; *P* = 0.423, *n* = 6). In contrast, significantly fewer p75^{NGFR}-immunoreactive BFCNs were present in Ts65Dn at 12 months of age (2N = 1512 ± 112; Ts65Dn = 1214 ± 49; *P* = 0.046, *n* = 6) and at 18 months of age (2N = 1914 ± 123; Ts65Dn = 1463 ± 63; *P* = 0.028, *n* = 5). There was a significant decrease in the number of BFCNs in Ts65Dn mice between 6 and 12 months (*P* = 0.028). (*b*) Plots of the cross-sectional area of p75^{NGFR}-immunoreactive BFCNs (mean ± SEM) revealed no significant difference between control (2N, red line) and Ts65Dn mice (black) at 6 months of age (2N = 118.4 ± 2.5 μm^2; Ts65Dn = 117.9 ± 2.0; *P* = 0.872, *n* = 6). In contrast, p75^{NGFR}-immunoreactive BFCNs were significantly smaller in Ts65Dn mice at 12 months of age (2N = 119.13 ± 2.9 μm^2; Ts65Dn = 110.2 ± 2.1; *P* = 0.038, *n* = 6) and at 18 months of age (2N = 139.5 ± 1.5 μm^2; Ts65Dn = 118.8 ± 4.5; *P* = 0.009, *n* = 5). There was a significant decrease in the cell profile area in Ts65Dn BFCNs between 6 and 12 months (*P* = 0.016). The significance of differences between Ts65Dn and 2N mice for values in this and all subsequent figures was determined either by the Kruskal–Wallis test (multiple comparisons) or the Mann–Whitney test (paired comparisons).

SEM; 2N = 137.3 ± 4.7 μm; *P* = 0.126, *n* = 3), but the width of this layer did differ at 18 months of age (Ts65Dn = 141.4 ± 2.9 μm; 2N = 154.6 ± 3.9 μm; *P* = 0.028, *n* = 5) because of a 12.5% increase in 2N animals and a 5.6% decrease in Ts65Dn relative to the values recorded at 6 months of age.

We then examined quantitatively the distribution and density of p75^{NGFR} immunoreactivity. There was no difference in the pattern of immunostaining for Ts65Dn and 2N subjects at age 6 months (Fig. 2 *e* and *g*). However, there was an overall increase in immunostaining of ≈38% in Ts65Dn mice at this age (optical density mean ± SEM; Ts65Dn = 121.2 ± 4.5; 2N = 88.1 ± 3.8; *P* = 0.003, *n* = 3). Because the thickness of the molecular layer did not differ between Ts65Dn and 2N mice at 6 months, this measurement points to an overall increase of cholinergic terminal immunostaining in Ts65Dn at this age. In quantitative studies on 18-month-old subjects, we confirmed the presence of a band of increased p75^{NGFR} immunostaining in the inner aspect of the molecular layer in Ts65Dn mice (Fig. 2 *f* and *h*). Of note, this band was similar to one seen in both Ts65Dn and 2N subjects at 6 months of age (compare Fig. 2*d* to *a* and *b*). In addition, there was a relative decrease in immunostaining in the outer aspect of this layer in aged Ts65Dn subjects (Fig. 2*f*), resulting in an overall decrease relative to 2N mice of 11% (Ts65Dn = 105.6 ± 5.8; 2N = 119.1 ± 4.2; *P* = 0.021, *n* = 5). This finding is evidence of an overall decrease in immunostaining of cholinergic terminals in the molecular layer of aged Ts65Dn mice.

Failed NGF Retrograde Transport in Ts65Dn Mice. Because neurotrophins, and NGF in particular, play an important role in regulating BFCN phenotype (9), and because findings analogous to those reported here are seen in animal models in which NGF production or signaling has been specifically disrupted (10–13),
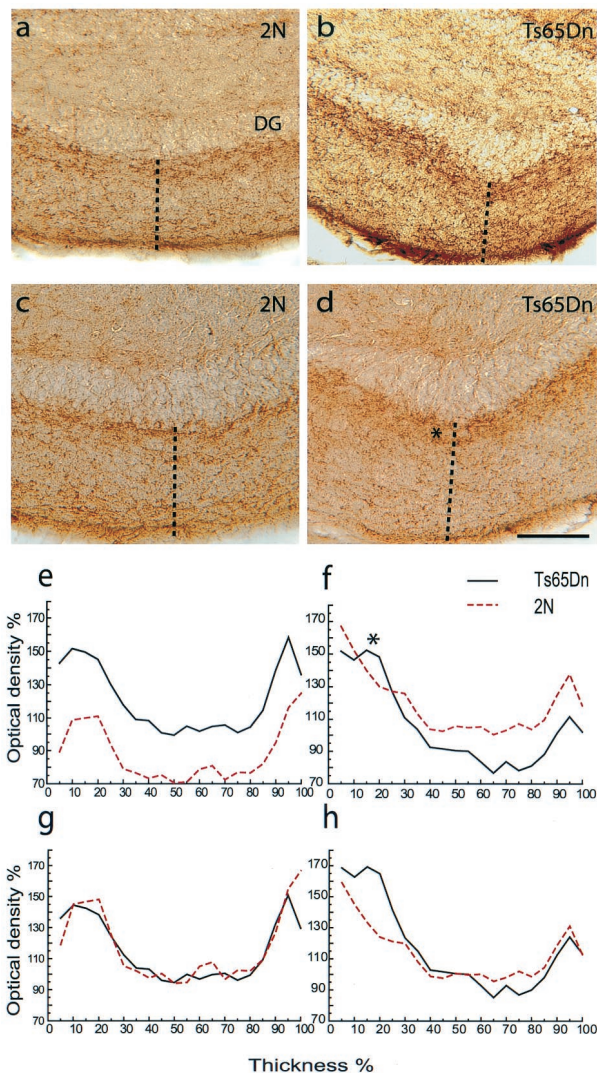

Fig. 2. Changes in the hippocampal terminal fields of BFCNs in Ts65Dn mice. Representative photomicrographs of p75^{NGFR}-immunoreactive fibers in the molecular layer adjacent to the inferior blade of the dentate granule cell layer (DG) in 6-month-old control (2N, *a*) and Ts65Dn (*b*) mice and in 18-month-old 2N (*c*) and Ts65Dn (*d*) mice. Note the dense layer of immunoreactive fibers immediately ventral to the dentate granule cell layer at 6 months in 2N and Ts65Dn mice and at 18 months in Ts65Dn mice (*). The dotted lines denote the position of representative optical slices used to quantitatively measure p75^{NGFR}-immunoreactive fibers. Scale bar is 50 μm. (*e* and *f*) Plots of binned optical density measurements for p75^{NGFR}-immunoreactive fibers in the molecular layer (% thickness starts immediately adjacent to the dentate granule cell layer). The optical density in Ts65Dn (black) was higher than in 2N mice (2N, dotted red line) at 6 months and lower than 2N at 18 months. In *g* and *h*, to better compare the patterns of fiber distribution, the data shown in *e* and *f* were normalized by setting as the 100% value the optical density measurement that was registered most frequently in each group.

we questioned whether changes in these parameters could underlie the abnormal phenotypes of p75^{NGFR}-positive BFCNs in Ts65Dn. NGF is produced and released in the hippocampus and binds to its receptors on the axon terminals of BFCNs before internalization and retrograde transport of NGF–NGF receptor complexes to the cell bodies of BFCNs (9). We began by examining NGF levels via ELISA in the hippocampus and septum of 2N and Ts65Dn mice at 6 and 12 months of age (Fig. 3). We noted a significant increase in NGF levels in the hippocampus of both 2N and Ts65Dn mice between 6 and 12
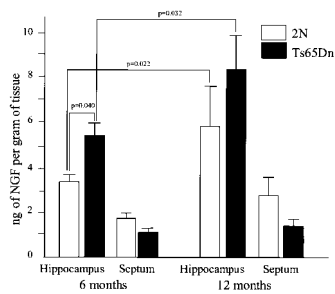
NEUROBIOLOGY

Fig. 3. Septal and hippocampal NGF levels in Ts65Dn mice. ELISA measurements of NGF (nanogram of NGF per gram of tissue, wet weight; mean ± SEM) showed significant increases in the hippocampus of both 2N and Ts65Dn mice between 6 and 12 months of age. NGF levels were significantly higher in the hippocampus of Ts65Dn (black) vs. 2N (white) mice at 6 months of age (2N = 3.4 ± 0.3; Ts65Dn = 5.5 ± 0.5, $P = 0.04$, $n = 5$) but were not significantly different at 12 months of age (2N = 5.9 ± 1.6; Ts65Dn = 8.7 ± 1.9; $P = 0.15$, $n = 4$). There was a trend toward a reduction in the level of NGF in the septal region of Ts65Dn mice at 6 months of age (2N = 1.7 ± 0.2; Ts65Dn = 1.0 ± 0.2; $P = 0.18$, $n = 5$) and at 12 months of age (2N = 3.0 ± 0.2; Ts65Dn = 1.4 ± 0.3; $P = 0.25$, $n = 4$), but these changes did not reach statistical significance.

months of age. Of note, hippocampal NGF levels were significantly higher in Ts65Dn mice than in 2N mice at 6 months of age. There was no significant difference between Ts65Dn and 2N mice at 12 months ($P = 0.15$). At both ages, Ts65Dn mice displayed a trend toward reduced NGF levels in the septal region, where BFCN soma are located, but the differences were not significant (6 months, $P = 0.18$; 12 months, $P = 0.25$). We conclude that NGF levels exceeded normal in the hippocampus of 6-month-old Ts65Dn mice.

An important test for evaluating NGF signaling is the ability of neurons to bind NGF in their target of innervation and to retrogradely transport NGF to their cell bodies (9). Increased NGF in the hippocampus of Ts65Dn mice at 6 months, without a corresponding increase in the septum, suggested a failure in retrograde transport of NGF and of the NGF signal in these mice. To investigate this possibility, we compared the retrograde transport of radiolabeled NGF injected into the hippocampus of 2N and Ts65Dn mice at 6 and 12 months of age (Fig. 4). In 2N mice of either age, a wave of radioactivity was observed moving from the hippocampus to the septum along the length of the fimbria at a rate of ≈2.0 mm/h, consistent with the rate of fast axonal transport. Conversely, Ts65Dn mice showed a noticeable transport defect in radiolabeled NGF at both 6 and 12 months of age. In fact, in Ts65Dn mice there was little or no significant retrograde transport of ^{125}I-NGF above background levels at any survival time. To address whether the defect in retrograde transport in Ts65Dn mice was specific for NGF, we performed similar experiments with radiolabeled BDNF and NT-3. However, using these methods we were unable to detect retrograde transport of either neurotrophin above background levels in the fimbria or septum of 2N mice (data not shown).

Decreased NGF transport could arise from failure of NGF to bind to its receptors on the axon terminals of BFCNs, from decreased internalization of NGF–NGF receptor complexes, or from defective retrograde trafficking of such complexes within axons to the cell bodies of BFCNs. To discriminate between these possibilities, we carried out studies of NGF binding and internalization in synaptosomes prepared from the hippocampuses of 6-month-old 2N and Ts65Dn mice. NGF binding was tested under conditions in which most high affinity and ≈50% of low affinity receptors would be occupied (9). There was no decrease in NGF binding in Ts65Dn synaptosomes (Table 1). Indeed, we consistently detected more binding in these preparations as compared with synaptosomes from 2N animals ($P <$
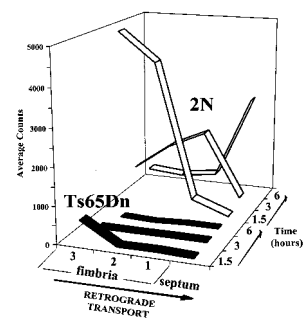

Fig. 4. Reduced retrograde transport of ^{125}I-NGF from hippocampus to BFCNs in Ts65Dn mice. Comparison of the retrograde transport of ^{125}I-NGF from the hippocampus to the septum via the fimbria in 2N (white) and Ts65Dn (black) mice at 6 months of age. Radiolabeled NGF was injected into the dorsal hippocampus. Following intervals of 1.5, 3, or 6 h, the hippocampus, fimbria, and septum were dissected, and the fimbria was subdivided as defined in *Materials and Methods*. In 2N mice, ^{125}I-NGF moved progressively in a wave through the proximal (i.e., closest to the hippocampus, fimbria 3), intermediate (fimbria 2), and distal segments (i.e., closest to the septum, fimbria 1) of the fimbria, arriving in the septum 6 h after injection. In contrast, in Ts65Dn mice there was little or no significant retrograde transport of ^{125}I-NGF above background levels. The results shown are those for individual mice of each genotype at each interval for sacrifice; the results at 6 h were confirmed in two additional mice of each genotype. Failure of retrograde transport was also found in 12-month-old Ts65Dn mice (data not shown).

0.005). Remarkably, NGF internalization was also increased in synaptosomes from Ts65Dn mice ($P < 0.05$). These data indicate that the defect in retrograde transport of NGF does not arise from a failure to bind or internalize NGF and suggest that it is because of an axonal abnormality that mediates retrograde transport.

NGF Infusion Reversed Cholinergic Neurodegeneration. We reasoned that if failed NGF retrograde signaling in Ts65Dn resulted in the smaller size and reduced the number of immunoreactive BFCNs, it may be possible to reverse these changes through bypassing retrograde transport. Therefore, we explored the effect of activating NGF receptors on BFCNs by delivering NGF directly to BFCN cell bodies through intracerebroventricular administration in Ts65Dn and 2N mice at 18 months of age (Fig. 5). NGF was found to completely reverse the atrophy of BFCNs immunoreactive for p75^{NGFR}, increasing their cross-sectional area (Fig. 5b). Indeed, NGF had a population-wide effect on the size of BFCNs in Ts65Dn mice (data not shown). These findings are evidence that even in aged Ts65Dn mice these neurons remain neurotrophin-responsive. More remarkably, NGF treatment also reversed the reduction in number of p75^{NGFR}-positive BFCNs in 18-month-old Ts65Dn mice (Fig. 5a), suggesting that these neurons did not die during aging but persisted in a state of phenotypic silence in which NGF-regulated markers were minimally expressed. Although we detected no change in the pattern of p75^{NGFR}-immunostained fibers with NGF treatment (data not shown), we did see an increase in the density of immunostaining

Table 1. NGF binding and internalization in hippocampal synaptosomes from 2N and Ts65Dn mice

Method*	2N	Ts65Dn	P values[†]
Surface bound before warming	31 ± 3.3	53 ± 2.6	<0.005
Internalization during warming	11 ± 1.5	14 ± 1.6	<0.05
Surface bound after warming	26 ± 0.6	39 ± 0.3	<0.05

*All results are expressed as pg of NGF per μg synaptosomes.
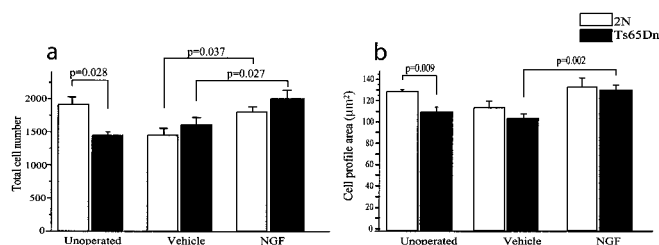[†]One-tailed t test. $n = 3$ for all measurements.

Fig. 5. Restoration of BFCN number and size by NGF infusion in aged Ts65Dn mice. Comparison of stereological data for the number (*a*) and size (*b*) of p75^{NGFR}-immunoreactive BFCNs in the MSN (mean ± SEM) of 18-month-old control (2N, white) and Ts65Dn (black) mice, either unoperated or after 2 weeks of continuous intracerebroventricular infusion of either NGF (0.9 μg/day) or artificial cerebrospinal fluid (vehicle). (*a*) Note that NGF treatment restored to normal the number of p75^{NGFR}-immunoreactive BFCNs in Ts65Dn (Ts65Dn, vehicle = 1612 ± 106, *n* = 8; Ts65Dn, NGF = 2004 ± 119, *n* = 8). NGF also reversed the decrease in number that accompanied vehicle treatment of 2N mice (2N, vehicle = 1450 ± 99, *n* = 6; 2N, NGF = 1805 ± 76, *n* = 6). (*b*) NGF treatment also significantly increased the cross-sectional area of p75^{NGFR}-immunoreactive BFCNs in Ts65Dn (Ts65Dn, vehicle = 104.7 ± 4.1 μm^2, *n* = 8; Ts65Dn, NGF = 131.7 ± 4.0, *n* = 8). NGF also increased the profile area of BFCNs in 2N mice by 17%, to the value seen in unoperated 2N mice (2N, vehicle = 115.1 ± 5.5, *n* = 6; 2N, NGF = 134.6 ± 8.4, *n* = 6). The difference was not statistically significant.

in both Ts65Dn and 2N mice. Significantly, following NGF treatment, the level of immunostaining in Ts65Dn subjects was the same as for 2N mice (P = 0.63). The change in cholinergic fiber density in response to NGF treatment is evidence that NGF treatment modified the terminal fields of aged BFCNs.

Discussion

Studies on DS patients suggest that BFCNs degenerate with increased age (3, 4, 22). This study significantly extends our previous work in demonstrating marked age-related abnormalities of BFCNs in Ts65Dn mice (6). We now provide evidence for two types of age-related abnormalities in these mice: one is the failure to show normal progressive changes; the other is the occurrence of regressive changes. Importantly, our findings suggest that both arise from defective transport of the NGF signal and that both can be reversed by treating BFCN cell bodies with NGF.

There was a marked failure of BFCNs in Ts65Dn mice to undergo the progressive changes in size and number that were seen in aged 2N mice. Although modest increases in these parameters were registered between 12 and 18 months, they were less marked than in 2N mice. As in the current study, in an earlier study (6) we detected no statistically significant difference in the number of BFCNs at 6 months, but a significant difference at 20 months. However, in the earlier study we failed to detect the increase in BFCN number with aging in 2N mice. This resulted from overestimating the number of 2N neurons at 6 months. For both cell number and cell size, our new results reflect significant improvements in experimental design, including the number of subjects examined and the use of a more sophisticated stereological system. Our findings in the 2N mice are consistent with age-related hypertrophy and apparent hyperplasia reported in the rat (23) and point to the possibility that normal aging results in the functional reorganization of cholinergic circuits that innervate the hippocampus. Although the mechanistic basis for these changes and their physiological significance are as yet unknown, given their trophic nature they may be in response to trophic alterations in the target of innervation, as suggested by the increase in hippocampal NGF levels seen during normal aging. Although the failure of BFCNs in Ts65Dn to show the normal increases in size and number could have been influenced

by changes in the hippocampus, it is most plausibly related to the abnormality in NGF retrograde transport demonstrated herein and thus to a defect(s) that is intrinsic to BFCNs.

Our studies show that a second, regressive component involved both cell bodies and axons of BFCNs in Ts65Dn mice. There was a significant decrease in both the size and number of BFCNs between 6 and 12 months in Ts65Dn subjects. These changes are especially remarkable given the increases that were registered at the same time in 2N mice. Evidence that a regressive component continued to affect BFCN cell bodies at later ages was the relatively ineffective increases in size and number registered between 12 and 18 months. In that decreased BFCN number has been found in cognitively impaired, but not normal, aged rodents (23, 24), our data are consistent with the finding of age-related impairments on tests of hippocampal function in Ts65Dn mice (8). The degenerative phenotypes exhibited by BFCN soma were accompanied by an overall decrease in p75^{NGFR}-immunoreactive fiber density in representative terminal fields of these neurons in the hippocampal formation. Although the functional significance of this change is yet to be defined, it suggests that there is dysfunction of cholinergic axon terminals, an assertion whose proof requires additional neurochemical and physiological studies.

Because NGF appears to be uniquely important for the development and maintenance of BFCNs (9–12), and because NGF signals through retrograde transport to act on BFCNs, we asked whether the atrophy and apparent loss of these neurons in Ts65Dn mice was because of a failure of NGF availability or of retrograde NGF signaling. Our finding of increased NGF in the hippocampus of Ts65Dn vs. 2N mice at 6 months of age suggested that decreased availability of NGF at BFCN terminals was not a factor. Hippocampal NGF mRNA or protein levels have similarly been reported as unchanged or even increased in AD patients (25, 26). NGF levels are reduced in the basal forebrain as a whole (26) and specifically within BFCNs (26, 27) in AD. Of note, we detected a trend toward decreased NGF levels in the septum of Ts65Dn mice. Failure to retrogradely transport target-derived NGF has been suggested, but not shown, to contribute to the degeneration of BFCNs in AD (28, 29). We investigated whether such a mechanism acts in Ts65Dn mice by examining NGF transport. Herein, we have provided a direct *in vivo* demonstration of the dynamics of fast retrograde axonal transport along a major fiber tract in the vertebrate central nervous system. Significantly, at the age of 6 months, we found that retrograde transport of radiolabeled NGF from the hippocampus to the basal forebrain was markedly decreased in Ts65Dn mice. The mechanistic basis for this defect is apparently related to the intracellular trafficking of NGF–NGF receptor complexes because, as demonstrated, neither NGF binding nor internalization was decreased. These studies provide strong evidence that retrograde NGF signaling is compromised in Ts65Dn mice. They demonstrate directly a failure in NGF retrograde transport in a model of DS or AD. Because the deficit in NGF transport was already severe in 6-month-old Ts65Dn, when no significant change in BFCN number or profile area was apparent, reduced availability of NGF may have resulted in a protracted process of BFCN degeneration. It is probable that these neurons are rendered more vulnerable by impaired retrograde NGF signaling (30, 31).

It has been hypothesized that reduced levels of TrkA expression by BFCNs contribute to the deficits in the number and size of these neurons in aged rats (30, 31) and AD subjects (28, 29). In this context, it is noteworthy that the number of TrkA-positive BFCNs is significantly reduced in 6-month-old Ts65Dn mice (7), an age when these mice exhibit almost complete failure of retrograde NGF transport. However, the hypothesis that TrkA levels play a critical role in the pathogenesis of BFCN dysfunction must be reexamined in view of our finding that retrograde

transport was defective when the axon terminal of BFCNs in Ts65Dn mice bound and internalized NGF as well as, or better than, those from 2N mice. Moreover, the robust response to exogenous NGF in aged BFCNs points to the existence of effective signal transduction pathways in neurons whose expression of TrkA and p75^{NGFR} is decreased. These data suggest strongly that failed NGF transport and signaling are more closely linked to abnormalities in BFCN function than are the observed reductions in the levels of NGF receptors.

The complete restoration of BFCN number and size by NGF treatment shows that it is possible to rescue these phenotypes in aged Ts65Dn, where abnormalities of cholinergic neuron structure and function are well established. This is compelling evidence for the ability of NGF to reverse pathological changes in a genetic model of DS with relevance to AD. Although the possibility exists that these findings could be because of stimulated neurogenesis among BFCN precursors, we know of no studies demonstrating the existence of such a population of cells in the basal forebrain. Nor is it likely that noncholinergic neurons of the basal forebrain were induced to take on the cholinergic phenotype; studies in rodents have shown that essentially all NGF receptor-expressing cells in the basal forebrain are cholinergic (14, 32). Thus, the NGF treatment effects are most plausibly interpreted as a reversal of phenotype in surviving BFCNs and are evidence that a population of these neurons does not die in Ts65Dn mice, as has been presumed. Instead, the reduction in the number of immunohistochemically detected BFCNs in Ts65Dn mice appears to represent dynamic down-regulation of these phenotypic markers. Earlier studies in aged rodents and aged primates also suggest that BFCNs can survive in a state of enduring "phenotypic silence" while remaining responsive to NGF (33, 34). Our study suggests that this state can arise from the failure to retrogradely traffic the NGF signal. That the terminals of BFCNs also responded to NGF treatment is consistent with recent findings in both rodents (35) and primates (34) and suggests that cholinergic terminals share in the beneficial effects of enhancing the trophic state of BFCN cell bodies.

Our findings have significant implications for understanding the pathophysiology of AD and DS and for the treatment of affected individuals. The failure in the trophic link between BFCNs and their targets of innervation in Ts65DN mice motivates studies to characterize the mechanism of retrograde signaling and its possible disruption in DS and AD. Understanding precisely the mechanism of the transport deficit and treating patients to reverse it may represent a method for ameliorating existing pathological changes. Of note, in an ongoing phase I trial of cell-mediated gene therapy, NGF is being delivered locally to the basal forebrain of AD patients (Mark Tuszynski, personal communication).

1. Whitehouse, P. J., Price, D. L., Struble, R. G., Clark, A. W., Coyle, J. T. & Delong, M. R. (1982) *Science* **215**, 1237–1239.
2. Mufson, E. J., Bothwell, M. & Kordower, J. H. (1989) *Exp. Neurol.* **105**, 221–232.
3. Casanova, M. F., Walker, L. C., Whitehouse, P. J. & Price, D. L. (1985) *Ann. Neurol.* **18**, 310–313.
4. Mann, D. M., Yates, P. O. & Marcyniuk, B. (1984) *Neuropathol. Appl. Neurobiol.* **10**, 185–207.
5. Reeves, R. H., Irving, N. G., Moran, T. H., Wohn, A., Kitt, C., Sisodia, S. S., Schmidt, C., Bronson, R. T. & Davisson, M. T. (1995) *Nat. Genet.* **11**, 177–184.
6. Holtzman, D. M., Santucci, D., Kilbridge, J., Chua-Couzens, J., Fontana, D. J., Daniels, S. E., Johnson, R. M., Chen, K., Sun, Y., Carlson, E., *et al.* (1996) *Proc. Natl. Acad. Sci. USA* **93**, 13333–13338.
7. Granholm, A. C., Sanders, L. A. & Crnic, L. S. (2000) *Exp. Neurol.* **161**, 647–663.
8. Hyde, L. A., Frisone, D. F. & Crnic, L. S. (2001) *Behav. Brain Res.* **118**, 53–60.
9. Sofroniew, M., Howe, C. & Mobley, W. C. (2001) *Annu. Rev. Neurosci.* **24**, 1217–1281.
10. Capsoni, S., Ugolini, G., Comparini, A., Ruberti, F., Berardi, N. & Cattaneo, A. (2000) *Proc. Natl. Acad. Sci. USA* **97**, 6826–6831.
11. Chen, K. S., Nishimura, M. C., Armanini, M. P., Crowley, C., Spencer, S. D. & Phillips, H. S. (1997) *J. Neurosci.* **17**, 7288–7296.
12. Li, Y., Holtzman, D. M., Kromer, L. F., Kaplan, D. R., Chua-Couzens, J., Clary, D. O., Knusel, B. & Mobley, W. C. (1995) *J. Neurosci.* **15**, 2888–2905.
13. Fagan, A. M., Garber, M., Barbacid, M., Silos-Santiago, I. & Holtzman, D. M. (1997) *J. Neurosci.* **17**, 7644–7654.
14. Koh, S. & Loy, R. (1989) *J. Neurosci.* **9**, 2999–3018.
15. Cooper, J. D., Messer, A., Feng, A. K., Chua-Couzens, J. & Mobley, W. C. (1999) *J. Neurosci.* **19**, 2556–2567.
16. Gunderson, H. J. G. (1984) *Analysis of Organic and Biological Surfaces* (Wiley, London), pp. 477–506.
17. Franklin, K. B. J. & Paxinos, G. T. (1997) *The Mouse Brain: In Stereotaxic Coordinates* (Academic, San Diego).
18. Fernyhough, P., Diemel, L. T., Hardy, J., Brewster, W. J., Mohiuddin, L. & Tomlinson, D. R. (1995) *Eur. J. Neurosci.* **7**, 1107–1110.
19. Mobley, W. C., Rutkowski, J. L., Tennekoon G. I., Gemski, J., Buchanan, K. & Johnston, M. V. (1986) *Brain Res.* **387**, 53–62.
20. Grimes, M. L., Zhou, J., Beattie, E. C., Yuen, E. C., Hall, D. E., Valletta, J. S., Topp, K. S., LaVail, J. H., Bunnett, N. W. & Mobley, W. C. (1996) *J. Neurosci.* **16**, 7950–7964.
21. Cooper, J. D. & Sofroniew, M. V. (1996) *Neuroscience* **75**, 29–35.
22. Yates, C. M., Simpson, J., Gordon, A., Maloney, A. F., Allison, Y., Ritchie, I. M. & Urquhart, A. (1983) *Brain Res.* **280**, 119–126.
23. Armstrong, D. M., Sheffield, R., Buzsaki, G., Chen, K. S., Hersh, L. B., Nearing, B. & Gage, F. H. (1993) *Neurobiol. Aging* **14**, 457–470.
24. Stemmelin, J., Lazarus, C., Cassel, S., Kelche, C. & Cassel, J.-C. (2000) *Neuroscience* **96**, 275–289.
25. Goedert, M., Fine, A., Hunt, S. P. & Ullrich, A. (1986) *Brain Res.* **387**, 85–92.
26. Scott, S. A., Mufson, E. J., Weingartner, J. A., Skau, K. A. & Crutcher, K. A. (1995) *J. Neurosci.* **15**, 6213–6221.
27. Mufson, E. J., Conner, J. M. & Kordower, J. H. (1995) *NeuroReport* **6**, 1063–1066.
28. Mufson, E. J., Lavine, N., Jaffar, S., Kordower, J. H., Quirion, R. & Saragovi, H. U. (1997) *Exp. Neurol.* **146**, 91–103.
29. Salehi, A., Verhaagen, J., Dijkhuizen, P. A. & Swaab, D. F. (1996) *Neuroscience* **75**, 373–387.
30. Cooper, J. D., Lindholm, D. & Sofroniew, M. V. (1994) *Neuroscience* **62**, 625–629.
31. Lams, B. E., Isacson, O. & Sofroniew, M. V. (1988) *Brain Res.* **475**, 401–406.
32. Smith, D. E., Roberts, J., Gage, F. H. & Tuszynski, M. H. (1999) *Proc. Natl. Acad. Sci. USA* **96**, 10893–10898.
33. Hu, L., Cote, S. L. & Cuello, A. C. (1997) *Exp. Neurol.* **143**, 162–171.
34. Conner, J. M., Darracq, M. A., Roberts, J. & Tuszynski, M. H. (2001) *Proc. Natl. Acad. Sci. USA* **98**, 1941–1946.
35. Fischer, W., Wictorin, K., Bjorklund, A., Williams, L. R., Varon, S. & Gage, F. H. (1987) *Nature (London)* **329**, 65–68.